

Effect of internals and sparger design on mixing behavior in sectionalized bubble column

Yogesh K. Doshi, Aniruddha B. Pandit*

Chemical Engineering Division, Institute of Chemical Technology, University of Mumbai, Matunga, Mumbai 400019, India

Received 27 April 2005; received in revised form 16 July 2005; accepted 19 July 2005

Abstract

An experimental study has been carried out to investigate the effect of internals and sparger design on mixing time (θ_{mix}) and fractional gas hold-up (ε_G) in a batch mode sectionalized bubble column. Air and water were used as the gas–liquid phases, respectively. In the present work, sparger with the percent free area (% FA) of 0.136 and 0.6% has been used and the superficial gas velocity (V_G), liquid height to column diameter (H_c/D), percent free area of the sectionalizing plate was varied from 0.06 to 0.295 m s^{-1} , 3 to 4 and 4 to 23%, respectively. It was found that there is no significant effect of the sparger design on the mixing time but it does strongly depend on V_G , H_c/D and % FA of the sectionalizing plate. The one-dimensional dispersion model successfully predicts the tracer concentration profile and the longitudinal dispersion coefficient. Also, the effect of the presence of the electrolyte too has been studied by adding a known volume of the tracer solution (NaCl). Correlations have been developed for the estimation of the fractional gas hold-up, mixing time, longitudinal dispersion coefficient (D_L) and the intercell exchange velocity (u_B).

© 2005 Elsevier B.V. All rights reserved.

Keywords: Sectionalized bubble column; Sparger plate; Mixing time; Intercell exchange velocity; Longitudinal dispersion coefficient; Compartment model

1. Introduction

Bubble columns are very commonly used in industrial reactions for carrying out gas–liquid contacting operation. Ease of operation and absence of moving parts makes this equipment a popular choice. The important reactions include oxidation, hydrogenation, halogenations, hydroformylation, Fischer-Tropsch reaction, ozonolysis, carbonylation, alkylation, fermentation, wastewater treatment, etc. This kind of reactors also finds application in catalyzed reactions, coal treatment, absorption and bio-reaction.

Bubble column hydrodynamics is characterized by different liquid flow patterns depending on the gas flow rate and the earlier identified resulting homogeneous, transition and heterogeneous regimes [1–3]. Bubbles are uniformly distributed in the liquid when gas flow rate is low. Bubble size distribution is relatively well-defined and is controlled by the sparger type and is uniform through the column. This is known as a

homogeneous flow regime. However, this state is not maintained when the gas is sparged more rapidly (high superficial gas velocity (V_G)) through the column. Bubbles aggregate coalesce and large bubbles are formed and rise more rapidly than the small bubbles. This type of flow is referred to as heterogeneous and is more common as a result of the high gas rates frequently adopted in the industry. These two flow patterns are separated by a transition regime that corresponds to the development of local liquid circulation pattern in the column which establishes in the heterogeneous regime. The gas passing upward through the reactor in the form of bubbles entrain liquid with it, which then proceed to move downwards again after the disengagement of the bubble at the top, forming a distinctive liquid circulatory pattern. Thus, an intense liquid circulation is developed which is responsible for fluid mixing and the generated liquid velocities enhance the heat and mass transport processes. In this case (heterogeneous regime), most of the gas is transported through the reactor in the form of large fast-ascending bubbles, with few small bubbles, remaining (trapped) in the circulating liquid. The conversion of the gas phase reactant, achieved in the

* Corresponding author. Tel.: +91 22 2414 5616; fax: +91 22 2414 5614.
E-mail address: abp@udct.org (A.B. Pandit).

Nomenclature

A_R	arithmetic average of free area of the sectionalizing plates
A_{RS}	arithmetic average plates free area including sparger
C	tracer concentration (gm L^{-1})
C_E	equilibrium concentration of tracer (gm L^{-1})
C_i	initial concentration of tracer (gm L^{-1})
D	diameter of the column (m)
D_A	arithmetic average of hole diameter of the sectionalizing plate (m)
D_{AS}	arithmetic average of plates hole diameter including sparger (m)
D_L	longitudinal dispersion coefficient in liquid phase ($\text{m}^2 \text{s}^{-1}$)
D_0	diameter of hole (mm)
FA	free area
g	acceleration due to gravity (m s^{-2})
H_c	clear liquid height in column (m)
H_D	dispersed liquid height (m)
n	number of plates including sparger
N	number of holes on the sectionalizing plate
S	H_c/D ratio
t	time (s)
u_B	intercell exchange velocity (m s^{-1})
$V_{b\infty}$	terminal bubble rise velocity (m s^{-1})
V_G	superficial gas velocity (m s^{-1})
Z	longitudinal distance between injection probe and slow response probe (m)
θ_{mix}	mixing time (s)
<i>Greek letters</i>	
ε_G	fractional gas hold-up
λ	liquid height filled with tracer

heterogeneous operating range is almost always lower than obtained from the homogeneous regime due to lower gas phase mean residence time and relatively lower gas–liquid interfacial area due to the bubble coalescence. Heterogeneous state and its consequent adverse effect on the space–time yields can be minimized by taking measures such as fitting perforated plates (internals) or incorporating special gas distributors, which extend the operating homogeneous regime to higher superficial gas velocity.

In spite of the wide variety of contact schemes induced in this equipment by means of the introduction of the internals such as perforated plates, baffles and other geometric irregularities, most of the work in this field has been carried out in equipment (bubble column) lacking these internals. The introduction of the internals intensifies mass transfer by reducing the fraction of larger bubbles by re-breaking them and also reducing the back mixing in both the phases. Therefore, the objective of this work was to study experimentally

the hydrodynamic behavior of the gas–liquid system in a bubble column provided with perforated plate as a sectionalizing plate with different free areas.

Liquid phase mixing time (θ_{mix}) is an important performance parameter when the bubble column operates in a batch mode. Knowledge of the mixing time gives information regarding the liquid phase back mixing characteristics and the liquid phase flow pattern. The knowledge of the flow pattern and associated liquid circulation velocities help in the determination of the concentration gradient deciding local and overall rates of the reaction and also the transport processes responsible for heat and mass transfer coefficient in the bubble columns.

Hydrodynamics parameters and phase mixing are strongly dependent on the flow structure and the corresponding pattern. Hence, the primary objective of this work is to perform an experimental study of the measurement of the mixing time and the fractional gas hold-up (ε_G) in a sectionalized bubble column, which are strongly influenced by the variation in the parameters, such as V_G , liquid height to column diameter (H_c/D), percent free area (% FA) of the sectionalizing plate.

2. Experimental

The experimental studies were carried out in a perspex cylindrical sectionalized bubble column (0.41 m i.d. and 2.87 m height) operated in a semi batch mode with air and water as working fluids. The gas sparger having 0.136 and 0.6% FA has been used in the present work. Weeping of liquid was observed for the gas sparger having 0.6% FA, hence the lowest superficial gas velocity chosen for this sparger was equal to 0.119 m s^{-1} to avoid weeping. Thus, the V_G was varied in the range $0.06\text{--}0.295 \text{ m s}^{-1}$ (for 0.136% sparger FA) and $0.119\text{--}0.295 \text{ m s}^{-1}$ (for 0.6% sparger FA). The H_c/D and the % FA of the sectionalizing plates were varied in the range of 3–4 and 4–23%, respectively for both the spargers. An aqueous solution of NaCl (5 M) was employed as a tracer. The volume of the tracer in each run was 200–400 ml depending on the H_c/D ratio to maintain tracer volume to liquid volume ratio within 0.002 to eliminate the tracer volume effect [4]. The details pertaining to the perforated plate geometry, configuration and the tracer volume injected during each run are as shown in Tables 1 and 2.

During the start of the experiment, no weep condition was achieved by first sparging the air through a precalibrated rotameter and then filling the column with water up to a desired clear liquid height (H_c) (which is measured by using side arm connected to the column) and was also noted immediately after the disengagement of the gas when the gas flow was stopped. In the presence of continuous gas bubbling, the liquid level fluctuates to make accurate measurements of the dispersed liquid height (H_D) difficult. This difficulty is overcome by noting the H_D at two positions (diametrically opposite) simultaneously by using scale attached to the column. Joshi et al. [5] described bed expansion method to

Table 1
Geometric configuration of sectionalized bubble column with sparger free area 0.136%

Set	H_c/D	Details	Plate position from bottom to top					Tracer (ml)	
			Bottom	1st	2nd	3rd	4th		5th
S1	3	% FA	0.136	4	4	4			200
		D_0 (mm)	3	5	5	5	–	–	
		N	25	269	269	269			
S2	4	% FA	0.136	4	4	4	4		400
		D_0 (mm)	3	5	5	5	5	–	
		N	25	269	269	269	269		
S3	3	% FA	0.136	4'	4'	4'			200
		D_0 (mm)	3	10	10	10	–	–	
		N	25	61	61	61			
S4	4	% FA	0.136	4'	4'	4'	4'		400
		D_0 (mm)	3	10	10	10	10	–	
		N	25	61	61	61	61		
S5	3	% FA	0.136	8	8	8			200
		D_0 (mm)	3	5	5	5	–	–	
		N	25	537	537	537			
S6	4	% FA	0.136	8	8	8	8		400
		D_0 (mm)	3	5	5	5	5	–	
		N	25	537	537	537	537		
S7	3	% FA	0.136	13	13	18.5			200
		D_0 (mm)	3	6	6	7	–	–	
		N	25	607	607	617			
S8	4	% FA	0.136	13	13	18.5	18.5		400
		D_0 (mm)	3	6	6	7	7	–	
		N	25	607	607	617	617		
S9	3	% FA	0.136	18.5	18.5	23			200
		D_0 (mm)	3	7	7	8	–	–	
		n	25	617	617	604			
S10	4	% FA	0.136	18.5	18.5	23	23		400
		D_0 (mm)	3	7	7	8	8	–	
		n	25	617	617	604	604		

estimate the value of ε_G and is as follows:

$$\varepsilon_G = \frac{H_D - H_C}{H_D} \quad (1)$$

The tracer was injected (injection time ~ 2 – 3 s) into the bottommost section of the column. Conductivity monitoring system, consisting of four conductivity probes (diameter 10 mm, response time of the probe less than 1 s), a conductivity meter, an ADC/DAC converter and a computer was used to acquire the changing conductivity data at a sampling frequency of 10 Hz and at a time interval of 1 s for update (average of 10 readings). The locations of conductivity probes are shown in Fig. 1. A typical conductivity response of the probe in the sectionalized bubble column is shown in Fig. 2. In the experiments termed as a single run, each time, for each values of V_G , fresh water was used to measure the mixing time and the fractional gas hold-up. In order to study the effect of the presence of the electrolyte due to the continued addition of the tracer on the mixing time and the fractional gas hold-up, a continuous run was also conducted. In the experiments termed as a continuous run, same water was used with repeated tracer

addition over the entire range of V_G studied in this work. In order to assess the flow resistance to exchange offered by the sectionalizing plate, pressure drop across each of the sectionalizing plate was measured using U-tube manometer filled with carbon tetrachloride as shown in Fig. 1.

The conductivity variation with respect to time was smoothened in order to remove noise present due to an occasional gas bubble in contact with conductivity probes and then used for the calculation of the various parameter such as mixing time, the liquid dispersion coefficient (D_L) and the intercell (inter compartmental) exchange velocity (μ_B).

Mixing time has been defined as the time required for achieving 95% homogeneity. Kasat and Pandit [6] have described the details for the calculation of 95% mixing time. The mixing time was calculated from the normalized conductivity versus time data of the slowest responding probe (which is placed at the top of column) for 95% homogeneity. The values of the experimental mixing time with respect to various parameters, reported later in the text are typically an average of 2–3 such experiments. Mixing time measurement was found to be reproducible within the accuracy of $\pm 10\%$.

Table 2
Geometric configuration of sectionalized bubble column with sparger free area 0.6%

Set	H_c/D	Details	Plate position from bottom to top					Tracer (ml)	
			Bottom	1st	2nd	3rd	4th		5th
S11	3	% FA	0.6	4	4	4			200
		D_0 (mm)	2	5	5	5	–	–	
		N	251	269	269	269			
S12	4	% FA	0.6	4	4	4	4		400
		D_0 (mm)	2	5	5	5	5	–	
		N	251	269	269	269	269		
S13	3	% FA	0.6	4'	4'	4'			200
		D_0 (mm)	2	10	10	10	–	–	
		N	251	61	61	61			
S14	4	% FA	0.6	4'	4'	4'	4'		400
		D_0 (mm)	2	10	10	10	10	–	
		N	251	61	61	61	61		
S15	3	% FA	0.6	8	8	8			200
		D_0 (mm)	2	5	5	5	–	–	
		N	251	537	537	537			
S16	4	% FA	0.6	8	8	8	8		400
		D_0 (mm)	2	5	5	5	5	–	
		N	251	537	537	537	537		
S17	3	% FA	0.6	13	13	18.5			200
		D_0 (mm)	2	6	6	7	–	–	
		N	251	607	607	617			
S18	4	% FA	0.6	13	13	18.5	18.5		400
		D_0 (mm)	2	6	6	7	7	–	
		N	251	607	607	617	617		
S19	3	% FA	0.6	18.5	18.5	23			200
		D_0 (mm)	2	7	7	8	–	–	
		N	251	617	617	604			
S20	4	% FA	0.6	18.5	18.5	23	23		400
		D_0 (mm)	2	7	7	8	8	–	
		n	251	617	617	604	604		

Joshi [7] has reported the equation for estimation of the value of u_B in a bubble column reactor as follows :

$$u_B = 0.4\{gD(V_G - \varepsilon_G V_{b\infty})\}^{1/3} \quad (2)$$

whereas, in the case of the sectionalized bubble column, the value of u_B is likely to be very different than that predicted by the above Eq. (2). Pandit and Joshi [8] have indicated that u_B values reduce substantially (proportionality constant reduces from 0.4 to 0.12) with the addition of the radial baffle as a sectionalizing device. Hence, a computer code was developed to estimate the u_B values for sectionalized bubble column and has been calculated by fitting the tracer concentration behavior by the compartment model with appropriate values of u_B as an adjustable parameter.

In a compartmental model, the column is theoretically divided into specific number of compartments, depending on the number of sectionalizing plates and the H_c/D ratio used. Uniform mixing within the individual compartments and liquid transfer between the adjacent compartments (inter-cell exchange velocity, μ_B) have been assumed to control the overall homogenization process [9].

In the case of sectionalized bubble column, each section acts as a CSTR. Rising gas bubbles, which entrain liquid and carry it upward, mainly causes the liquid phase dispersion. Gas phase dispersion intensifies due to bubble breakage and coalescence at each sectionalizing plate, producing really wide residence time distributions in the gas phase due to a differential bubble rise velocities. This differential bubble rise velocity and gas hold-up distribution is responsible for the liquid phase dispersion and mixing, which in turn affect the gas-phase dispersion. Deckwer [10] has suggested that the radial dispersion coefficient is always less than one-tenth of the value of the axial dispersion coefficient. Therefore, one-dimensional (axial) model is sufficient to mimic the liquid phase mixing phenomena in a sectionalized bubble column and the longitudinal dispersion coefficient can then be used to express the liquid phase back-mixing characteristic of the bubble column. Also, Deckwer [10] has reported that the one-dimensional model can be applicable to both steady state and non-steady state (batch mode) measuring methods. Ohki and Inoue [11] have reported the basic equation of one-dimensional diffusion model for a semi-batch mode, which

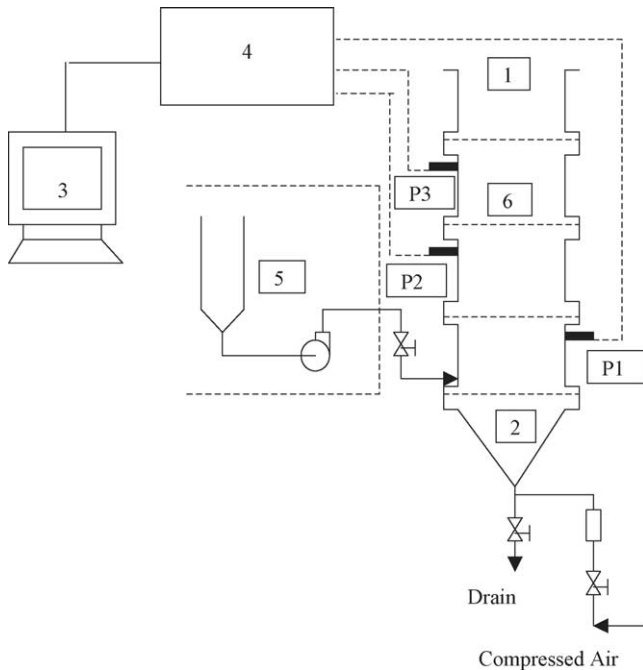


Fig. 1. Schematic diagram of experimental set-up

1	Sectionalized bubble column
2	Air chamber
3	Computer
4	Conductivity monitoring system
5	Tracer injection assembly
6	sectionalizing plate (perforated plate)
P1	Probe located at the bottom section
P2	Probe located at intermediate position
P3	Probe located at the top i.e. slowest response probe

is as follows:

$$\frac{C}{C_E} = 1 + 2 \sum_{n=1}^{\infty} \left[\cos \left(\frac{n\pi Z}{H_D} \right) \exp \left(- \left(\frac{n\pi}{H_D} \right)^2 D_L t \right) \right] \quad (3)$$

Eq. (3) has been used for modeling of the tracer movement to match (with appropriate D_L in Eq. (3)) the observed experimental tracer response. The experimental and predicted values of the conductivity variation (with appropriate value of D_L) as a function of time gave a good match with the experimental values as shown in Fig. 2.

3. Result and discussion

3.1. Fractional gas hold-up

3.1.1. Effect of superficial gas velocity

A significant increase in the fractional gas hold-up has been observed with an increase in the superficial gas velocity (Tables 3 and 4) as expected. For lower range of V_G , the increase in the gas hold-up is around 25% and this increment goes down with an increase in the V_G . Kemoun et al. [12] have observed similar behavior of gas hold-up with superficial gas velocity in a trayed bubble column. In the present work, with sectionalized bubble column around 33% fractional gas hold-up value was observed for the highest value of V_G (0.295 m s^{-1}) and for lowest free area of the sectionalizing plate in against 22% without sectionalization.

At low superficial gas velocities, the bubbles are uniformly dispersed along the column diameter and travel through the plate without much hindrance. An increase in the gas velocity enhances bubble coalescence due to their increased number density below the sectionalizing plate. Bubbles accumulate below the sectionalizing plate and are then redistributed. These bubble pockets go on increasing in

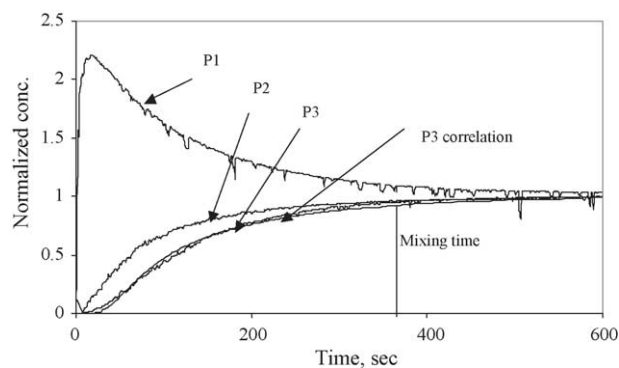


Fig. 2. Conductivity responses of the different probes for sectionalized bubble column

P1	indicate the response from probe 1 located at 0.38 m from bottom (i.e. in first section).
P2	indicate the response from probe 2 located at 0.76 m from bottom.
P3	indicate the response from probe 3 located at the top i.e. slowest response probe.
P3 correlation	indicates the predicted response for P3 using Equation (3).

Table 3
Variation in the fractional gas hold-up for sectionalized bubble column with $H_c/D = 3$

Free area	V_G (m/s)	Fractional gas hold-up			
		Single run ^a	Continuous run ^a	Single run ^b	Continuous run ^b
4, 4, 4	0.062	0.109	0.109	–	–
	0.089	0.152	0.155	–	–
	0.119	0.199	0.201	0.200	0.200
	0.149	0.231	0.236	0.232	0.237
	0.181	0.259	0.272	0.259	0.274
	0.217	0.289	–	0.285	0.296
4', 4', 4'	0.062	0.104	0.104	–	–
	0.089	0.140	0.144	–	–
	0.119	0.179	0.184	0.188	0.188
	0.149	0.213	0.225	0.228	0.232
	0.181	0.244	0.265	0.259	0.272
	0.217	0.271	–	0.283	0.299
8, 8, 8	0.062	0.105	0.105	–	–
	0.089	0.141	0.146	–	–
	0.119	0.183	0.185	0.188	0.188
	0.149	0.218	0.222	0.217	0.219
	0.181	0.244	0.252	0.243	0.249
	0.217	0.267	0.276	0.269	0.279
13, 13, 18.5	0.062	0.109	0.109	–	–
	0.089	0.135	0.138	–	–
	0.119	0.172	0.180	0.195	0.195
	0.149	0.208	0.217	0.220	0.224
	0.181	0.232	0.248	0.247	0.250
	0.217	0.266	0.281	0.267	0.274
18.5, 18.5, 23	0.062	0.110	0.110	–	–
	0.089	0.140	0.149	–	–
	0.119	0.177	0.184	0.187	0.187
	0.149	0.208	0.220	0.213	0.217
	0.181	0.228	0.252	0.232	0.237
	0.217	0.252	0.281	0.255	0.268
18.5, 18.5, 23	0.252	0.278	0.303	0.273	0.283
	0.295	0.294	–	0.289	–

^a Sparger free area = 0.136%.

^b Sparger free area = 0.6%.

their size with an increase in the gas velocity and they have a major contribution towards the increase in the fractional gas hold-up, though in terms of the gas liquid mass transfer these gas pockets may not have any significant contribution.

3.1.2. Effect of H_c/D ratio

For the higher range of V_G , there is about 9% increase in the fractional gas hold-up value with an increase in the H_c/D from 3 to 4 for both the spargers. It was also observed that there is no effect of H_c/D ratio on the differential pressure drop across the sectionalizing plates indicating there is no additional energy dissipation and hence, no possible additional bubble break-up causing an increase in the fractional gas hold-up. This suggests that an observed increase in

the fractional gas hold-up can mainly be attributed to the gas pockets formed below the additional sectionalizing plate.

3.1.3. Effect of % FA of the sectionalizing plate

Besides V_G and H_c/D ratio, fractional gas hold-up was also found to depend on the % FA of the sectionalizing plate, where one observes the variation in the fractional gas hold-up for both the spargers and for all the operating conditions. It is clear that the fractional gas hold-up for lower free area of the sectionalizing plate is higher, whereas in the case of same free area, number of holes has also an effect on the gas hold-up. In the present work, with the decrease in the free area from 23 to 4% there is a maximum increase of 15% in the gas

Table 4
Variation in the fractional gas hold-up for sectionalized bubble column with $H_c/D = 4$

Free area	V_G (m/s)	Fractional gas hold-up			
		Single run ^a	Continuous run ^a	Single run ^b	Continuous run ^b
4, 4, 4, 4	0.062	0.119	0.119	–	–
	0.089	0.157	0.161	–	–
	0.119	0.187	0.208	0.197	0.197
	0.149	0.220	0.249	0.229	0.239
	0.181	0.247	0.292	0.260	0.275
	0.217	0.278	–	0.283	0.306
	0.252	–	–	0.304	0.331
4', 4', 4', 4'	0.062	0.109	0.109	–	–
	0.089	0.146	0.152	–	–
	0.119	0.185	0.192	0.189	0.189
	0.149	0.214	0.231	0.219	0.231
	0.181	0.239	0.270	0.248	0.265
	0.217	0.265	–	0.273	0.301
	0.252	0.303	–	0.301	–
8, 8, 8, 8	0.062	0.107	0.107	–	–
	0.089	0.143	0.143	–	–
	0.119	0.183	0.189	0.189	0.189
	0.149	0.217	0.223	0.221	0.226
	0.181	0.241	0.258	0.244	0.258
	0.217	0.263	0.284	0.268	0.284
	0.252	0.282	–	0.287	0.310
13, 13, 18.5, 18.5	0.062	0.105	0.104	–	–
	0.089	0.148	0.146	–	–
	0.119	0.176	0.182	0.187	0.187
	0.149	0.208	0.221	0.218	0.221
	0.181	0.225	0.250	0.232	0.246
	0.217	0.250	0.278	0.252	0.271
	0.252	0.272	0.306	0.275	0.294
18.5, 18.5, 23, 23	0.062	0.114	0.114	–	–
	0.089	0.151	0.153	–	–
	0.119	0.177	0.188	0.188	0.188
	0.149	0.207	0.226	0.215	0.221
	0.181	0.227	0.254	0.234	0.249
	0.217	0.250	0.283	0.253	0.275
	0.252	0.272	0.306	0.273	0.295
0.295	0.289	–	0.288	–	

^a Sparger free area = 0.136%.

^b Sparger free area = 0.6%.

hold-up and for constant free area of 4%, due to a decrease in the number of holes in the sectionalizing plate there is a decrease in the gas hold-up values by 3% at low value of V_G equals to 0.062 m s^{-1} and by 8% at high value of V_G equals to 0.295 m s^{-1} . Kemoun et al. [12] has observed similar effect and has reported similar trend. An increased pressure drop (Table 5) across the sectionalizing plates with reduced free area (higher local energy dissipation rate) also contribute to the more efficient bubble break-up, reducing its average size and hence an increase in the gas hold-up. Also, an increase in the thickness of the accumulated gas pockets below the sectionalizing plate with a reduction in the % FA has been observed [13]. This could also be one of the possible reasons

for an observed increase in the overall gas hold-up with decreasing % FA.

3.1.4. Effect of the presence electrolyte

Due to the repetitive addition of an electrolyte (as a tracer solution) bubble coalescence decreases (the system becomes a non-coalescing one), reducing the average bubble diameter and hence increasing the fractional gas hold-up as compared to that in a single run. In other words, one can say that, a higher gas hold-up is caused by the retention of finely dispersed bubbles due to their non-coalescence. Due to the presence of electrolyte, there was an increase in the fractional gas hold-up (by 1–10%) in the case of a continuous run depending

Table 5
Pressure drop across the sectionalizing plates

Sparger free area	Sets	V_G (m/s)							
		0.062	0.089	0.119	0.149	0.181	0.217	0.252	0.295
0.136	S1, S2			1107	1256	1362	1495	1581	1660
	S3, S4			1217	1404	1588	1746	–	–
	S5, S6			1067	1154	1348	1436	1530	–
	S7, S8			930	1087	1107	1303	1460	–
	S9, S10			981	1114	1220	1311	1491	–
0.6	S11, S12			1202	1310	1429	1610	1699	–
	S13, S14			1272	1510	1607	1774	1816	–
	S15, S16			1158	1220	1405	1535	1645	–
	S17, S18			984	1161	1323	1480	1618	–
	S19, S20			1052	1205	1340	1495	1630	–

upon the V_G over the observation made in the case of a single run. Kelkar et al. [14] have also observed an increase in the gas hold-up with the addition of electrolyte and at low electrolyte concentrations; the increase was of the similar order of magnitude.

3.1.5. Effect of sparger free area

The fractional gas hold-up for a sectionalized bubble column with different sparger free areas showed only a small variation. Over the entire range of V_G , with an increase in the free area of the sparger from 0.136 to 0.6%, there was maximum 2% increase in the fractional gas hold-up for higher free

area of the sectionalizing plate and this goes on increasing with an decrease in the % FA. This increment reaches up to 7% for lowermost free area sectionalizing plate used in the present work. Kemoun et al. [12] have reported that, with an increase in the number of holes in the sparger (with the same hole diameter) there is an increase in the overall fractional gas hold-up. In the present work, the possible reason for the observed increase in the fractional gas hold-up could be due to the combined effect of the decrease in the diameter of the sparger holes and increase in the number of the holes on the sparger plate, giving better gas distribution thereby reducing the extent of bubble coalescence.

The comparative studies reveal that the sectionalized bubble column offers higher fractional gas hold-up as compared to the bubble column. It was found that in the case of bubble column with 0.136% sparger free area, fractional gas hold-up values was 0.09, for low value of V_G (0.062 m s^{-1}) and in the case of sectionalized bubble column it was 0.11. Similarly, for highest V_G (0.295 m s^{-1}) it was found to be 0.22 in the case of bubble column and 0.33 in the case of sectionalized bubble column. The possible reason for an increase in the fractional gas hold-up in the case of the sectionalized bubble column could be due to the re-breakage of the bubbles, when they pass through each of the sectionalizing plates.

3.1.6. Correlation for fractional gas hold-up

It has been observed that, in both the cases (bubble column and sectionalized bubble column) superficial gas velocity, free area of the sectionalizing plates as well as the sparger plate, diameter of the holes on the sectionalizing plates as well as sparger and H_c/D ratio have a major effect on the fractional gas hold-up. Hence, it was thought desirable to have a generalized correlation with above said parameters to correlate the observed variation in the fractional gas hold-up for bubble column and the sectionalized bubble column. The proposed correlation also is applicable for both the spargers used in this study with a correlation coefficient equal to 0.95 and is as follows:

$$\varepsilon_G = \left(0.7 + \left(0.055 \times n - 0.43 \times A_{RS} - 0.48 \times \frac{D_{AS}}{D} - 0.055 \times S \right) \right) \times V_G^{0.63} \quad (4)$$

where, A_{RS} is the arithmetic average of plates free area including sparger, D_{AS} is the arithmetic average of the plates hole diameter including sparger, n is the number of plates including sparger and S is the H_c/D ratio. It can be seen from the parity plot (Fig. 3) for the correlation (Eq. (4)) that the agreement is reasonable (S.D. 7.26%) and the correlation essentially captures the effect of all the parameters. From the above said correlation it is clear that the superficial gas

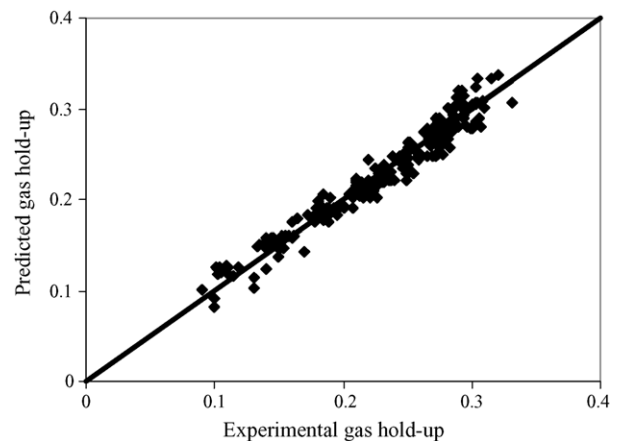


Fig. 3. Comparison of predicted gas hold-up with experimental.

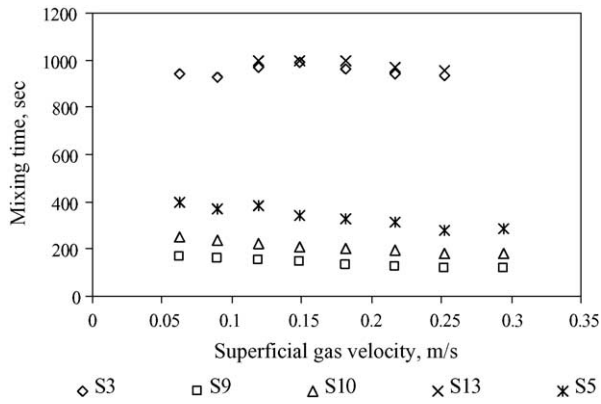


Fig. 4. Mixing time vs. superficial gas velocity with H_c/D , % free area of the sectionalizing plate and sparger free area as parameter.

velocity has a major contribution towards fractional gas hold-up along with free area of the plates and plates hole diameter.

3.2. Mixing time

3.2.1. Effect of superficial gas velocity

It can be seen from Fig. 4 that the mixing time decreases with an increase in the superficial gas velocity for the sets S3, S5, S9, S10 and S13. Similar type of trend was observed for all set except S4 (Fig. 5). With an increase in the superficial gas velocity, there is an increase in the exchange between cells causing a reduction in the mixing time. The current observed trend is consistent with the earlier report [15]. For set S4, there is an increase in the mixing time and it is possibly due to a decrease in the number of holes on the sectionalizing plate for set S4. Decrease in the number of holes reduces the intercell exchange velocity, which causes an increase in the mixing time. This has been explained in detail in the subsequent section.

3.2.2. Effect of H_c/D ratio

Fig. 4 also shows that mixing time increases with an increase in the H_c/D ratio for the sets S9 and S10, which is, as expected. Similar type of behavior was observed for

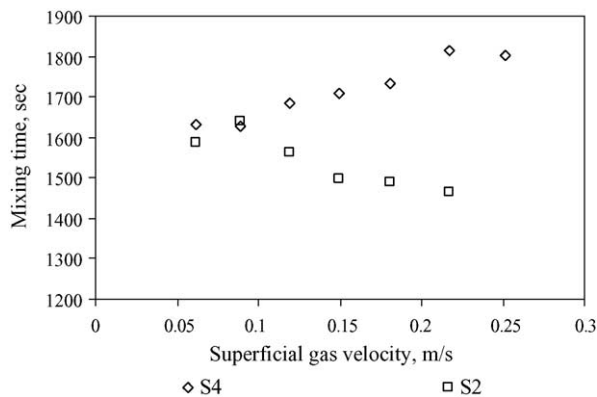


Fig. 5. Mixing time vs. superficial gas velocity with diameter of sectionalizing plate as parameter.

all the sets studied. An increase in the H_c/D ratio means an increase in the clear liquid height. The time required for the tracer to get homogenized over a longer distance and over a higher liquid volume also increases, causing an increase in the mixing time. In the present work, the increment in the mixing time is about 100% for low free area of the sectionalizing plate with an increase in H_c/D ratio from 3 to 4.

3.2.3. Effect of % FA of the sectionalizing plate

Due to the sectionalization, the multiple compartments are isolated from each other and each section behaves as a single CSTR with some intercell exchange velocities ' u_B ', which depends on the available free area of the sectionalizing plates in addition to the circulation velocities with each cell. With a decrease in the free area of the sectionalizing plate, the exchange between adjacent cells reduces causing to increase in the mixing time substantially. Due to a decrease in the free area (from 23 to 4%) of the sectionalizing plate, the intercell exchange velocity decreases (Fig. 6) and results in an increase in the mixing time (by almost 85%). Van Baten and Krishna [15] have also reported that intercell exchange velocity decreases from 0.014 to 0.0055 m s^{-1} with a decrease in the % FA of the sectionalizing plate from 30.7 to 18.6%.

3.2.4. Effect of the presence of electrolyte

Due to the repetitive addition of electrolyte (tracer), the system becomes non-coalescence type and the average bubble size reduces, causing an increase in the fractional gas hold-up (as discussed earlier). If we use the energy balance approach as proposed by Joshi [7] to explain this effect, one could argue that less energy is available for the liquid motion (as more energy gets dissipated at the gas–liquid interfacial area due to higher ϵ_G), thereby reducing the liquid circulation velocity and hence resulting in an increase in the mixing time as compared to the case of single run. The increment in the mixing time due to the addition of an electrolyte as compared to single run is as shown in Fig. 7 for the sets S9 and S10. This type of an increment is observed for all the sets of internals. In the present work, the observed increase in the mixing time

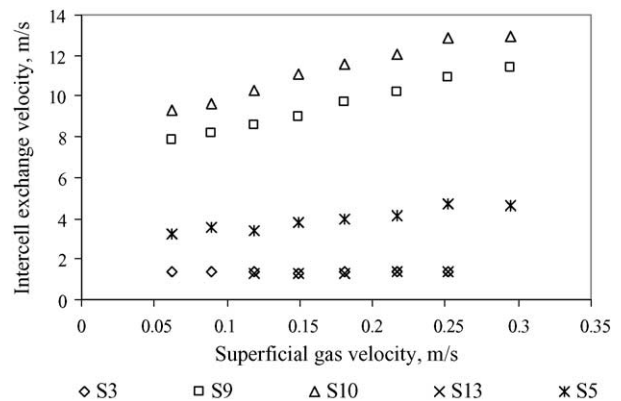


Fig. 6. Intercell exchange velocity vs. superficial gas velocity with H_c/D , % free area of the sectionalizing plate and sparger free area as parameter.

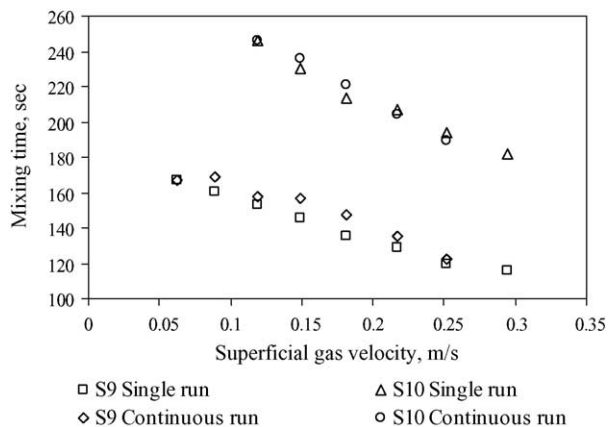


Fig. 7. Mixing time vs. superficial gas velocity with electrolyte concentration as parameter.

at identical V_G is from 1 to 22% for a decrease in the free area of the sectionalizing plate from 23 to 4%. Mixing time values obtained for a continuous run are consistent with the above argument, if one compares the increased ε_G values at identical V_G .

3.2.5. Effect of sparger free area

From Fig. 4, it was clear that there is no substantial change in the mixing time for the sets S3 and S13 over the range in the sparger free area covered in this work. This behavior was observed for all the sets of internals. In the case of the sectionalized bubble column, each sectionalizing plate acts as the sparger and hence the original gas sparging plate has very little or no contribution towards the overall mixing process even though there is a change in the sparger free area.

3.2.6. Correlation for mixing time

Following type of empirical correlation has been proposed to predict the variation in the mixing time as a function of number of plates including the sparger, superficial gas velocity, dispersion height, clear liquid height, plate hole diameter and free area of the plates including the sparger.

$$\theta_{\text{mix}} = (-0.98 + n^{2.15}) \times \left(\frac{V_G \times H_D (1 - 0.9 \times \varepsilon_G)}{H_C} \right)^{(D_{AS}/D) \times (-5.59)} \times A_{RS}^{-1.1} \quad (5)$$

The mixing time is a strong function of n and A_{RS} almost with a power of 2.15 and -1.1 , respectively. The negative power of A_{RS} clearly indicates inverse proportionality with mixing time and it has been already discussed in Section 3.2.3. The parity plot for the above said correlation is as shown in Fig. 8. The predicted values of mixing time from the above equation are in good agreement with the experimental values with S.D. of 15%. The proposed correlation is applicable for both the sparger plates studied in this work with a correlation coefficient R^2 equal to 0.97.

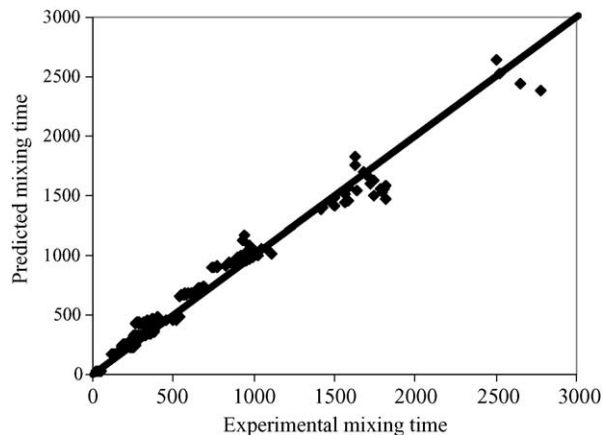


Fig. 8. Parity plot for mixing time.

3.3. Liquid phase dispersion coefficient

It can be seen from Fig. 9 that dispersion coefficient increases with an increase in the V_G for the sets S1, S11, S5, S9 and S10, which is consistent with the previous results [13]. The dispersion coefficient increases with an increase in the H_c/D ratio for the sets S9 and S10 (Fig. 9). The increment in the dispersion coefficient is smaller for lower free area (4% i.e. set S1) of the sectionalizing plate and goes on increasing with an increase in the free area (18.5% i.e. set S9) of the sectionalizing plate. This increase is from 1 to 7% for low free area and 3 to 14% for high free area. The possible reason for an increase in the dispersion coefficient is due to an increase in the H_c and H_D , which subsequently increases the mixing time (due to longer loop need to homogenization) at constant superficial gas velocity. There is also a significant increase in the dispersion coefficient with an increase in the free area of the sectionalizing plate for the sets S1, S5 and S9 (Fig. 9). An increase in the free area of the sectionalizing plate causes an increase in the back mixing due to a higher interaction between the adjacent sections, which is indicated by an increase in the dispersion coefficient. This result is

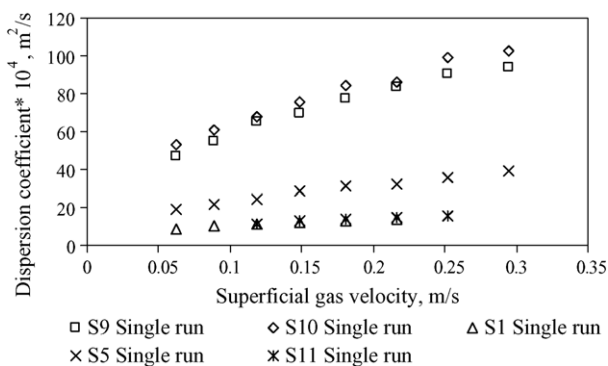


Fig. 9. Liquid phase dispersion coefficient vs. superficial gas velocity with H_c/D , % free area of the sectionalizing plate and sparger free area as parameter.

consistent with the previous results [13]. Due to an increase in the free area of the sectionalizing plate from 4 to 18.5%, dispersion coefficient value increases by almost 650% at high value of V_G . The dispersion coefficient for both the sparger for the sets S1 and S11 is also shown in Fig. 9 and is clear that there is no substantial change in the dispersion coefficient over the change in the sparger free area covered in this work. Similar behavior was observed for all the sets studied.

Field and Davidson [16] have reported the relationship between dispersion coefficient, dispersion height and mixing time as follows:

$$D_L = \left(\frac{A \times H_D^2}{\theta_{\text{mix}}} \right) \quad (6)$$

where A is 0.5. In the present work, it has been observed that the value of A is different and is a function of the arithmetic average of sectionalizing plate free area, sectionalizing plate hole diameter and superficial gas velocity. Hence, similar format to that of Eq. (6) with A as a function of the above said parameter has been used for the prediction of dispersion coefficient for bubble column and sectionalized bubble column. The new generalized correlation is as follows:

$$D_L = ((-0.7 + (1 + A_R)^{(D_A/D)^{0.5}}) \times V_G^{-0.22}) \times \left(\frac{H_D^{1.57}}{\theta_{\text{mix}}} \right) \quad (7)$$

where A_R is the arithmetic average of the free area of the sectionalizing plates, D_A is the arithmetic average of the hole diameters of the sectionalizing plates. The above said correlation is applicable for both the sparger plates used in this work with a correlation coefficient equal to 0.98. The predicted values of the dispersion coefficient from the above equation are in good agreement with experimental values with S.D. of 12%. The parity plot for the above said correlation is as shown in Fig. 10.

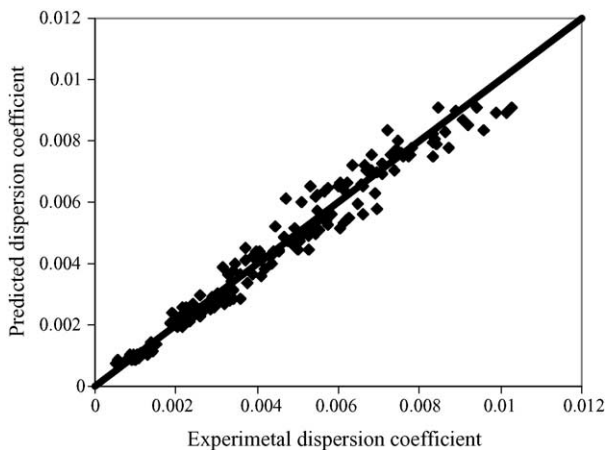


Fig. 10. Parity plot for dispersion coefficient.

3.4. Intercell exchange velocity

From Fig. 6, it is clear that the estimated intercell exchange velocity increases with an increase in the V_G for the sets S3, S5, S9, S10 and S13. An increase in the V_G is equivalent to an increase in the energy dissipation rate. This increasing energy dissipation has been used for increasing the liquid circulation velocities, which could result in an increase in the intercell exchange velocity and hence a decrease in the mixing time. Dreher and Krishna [13] have reported that the intercell exchange velocity increases with an increase in the superficial gas velocity. From Fig. 6, it is also clear that with an increase in the H_c/D ratio from 3 to 4 (i.e. sets S9 to set S10), there is an increase (around 20%) in the intercell exchange velocity even though there is an overall increase in the mixing time. This increase in the mixing time is due to an increase in the clear liquid height H_c . Thus, the energy available for the liquid motion could still be higher due to the reduced energy dissipation at the gas–liquid interface, resulting into higher liquid circulation velocities as per energy balance argument and also increased values of intercell exchange velocities. Fig. 6 clearly shows the suppression of the liquid phase back mixing being critically dependent on the free area of the sectionalizing plate. Fig. 6 clearly shows that with an increase in the free area of the sectionalizing plate from 4' to 18.5% (i.e. from the sets S3 to set S9) there is an increase in the u_B (around 650%). An increase in the free area of the sectionalizing plate obviously causes an increase in the exchange and hence in the back mixing which in turn helps to reduce in the mixing time. Dreher and Krishna [13] have also reported that with an increase in the free area of the sectionalizing plate there is an increase in the intercell exchange velocity. Similar behavior was observed for all the sets studied.

From Fig. 6, it can also be observed that there is no significant change in the intercell exchange velocity over the change in the sparger free area covered in this work (set S3 with sparger FA = 0.136% and set S13 with sparger FA = 0.6%).

To predict the intercell exchange velocity, Pandit and Joshi [8] have reported the following correlation for bubble column with radial baffle as follows:

$$u_B = \left(\frac{H_D}{\theta_{\text{mix}}} \right) \times \left(\frac{A}{\pi^2} \right) \left[S - \frac{B}{S + (C/S)} \right] \quad (8)$$

where the values of A , B and C are 2.85, -0.25 and -2.25 , respectively. In the present work, it has been observed that the value of A is 2.62 that is closer to 2.85, whereas the values of B and C are observed to be the functions of the arithmetic average of sectionalizing plate free area and the arithmetic average of hole diameter of the sectionalizing plates. Hence, similar format to that of Eq. (8) with B and C as functions of above said parameter has been used for the prediction of intercell exchange velocity for bubble column and sectionalized bubble column. The new generalized correlation is as

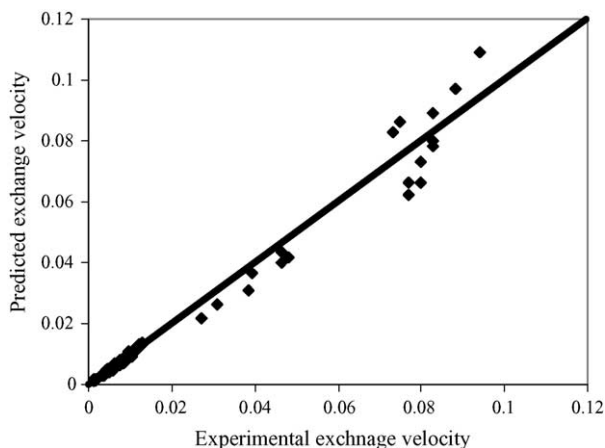


Fig. 11. Parity plot for intercell exchange velocity.

follows:

$$u_B = \left(\frac{H_D}{\theta_{\text{mix}}} \right) \times \left(\frac{2.62}{\pi^2} \right) \left[S - \frac{(D_A/D)^{(1+A_R)}}{S + ((D_A/D)^{(1+A_R)}/S)} \right] \quad (9)$$

The above said correlation is applicable for both the sparger plates used in this work with a correlation coefficient 0.98. The predicted values of intercell exchange velocity from the above equation are in good agreement with experimental work with S.D. of 7.7%. The parity plot for the above said correlation is as shown in Fig. 11.

3.5. Validation of correlations on the basis of literature data

The validation of the correlation based upon the data generated in the present case was carried out with the data reported by other researchers working on the sectionalized/partitioned bubble column. However, due to considerable difference in the system configuration variation in the predicted values was in the range of –28 to +44% for ε_G and 4 to 33% for the liquid phase dispersion coefficient, whereas in the case of some other publications the comparison was not possible because of inadequate experimental details supplied by the researchers.

The correlations developed in the present case are applicable for the system in which the distance between the adjacent sectionalizing plates is equal to the column diameter. Yamashita [17] has done work with partitioned plate similar to the present case. But positioning of the sectionalizing plate from the sparger is different than the present work. Dreher and Krishna [13] have not reported the clear liquid height (H_c) and hence the present correlation cannot be used to compare their data. The data of Kemoun et al. [12] and De [18] could be partially compared with the present correlations but there is quite deviation in the predicted values as the sectionalizing plate of Kemoun et al. [12] system has a 10% down comer area and only pipe gas sparger, whereas De [18] has used a single hole sparger and a loosely fitting stack of the sectionalizing plate

in the system. Also, operating range of superficial gas velocity is significantly different than used in the present case. All these variations results into the deviation observed during the comparison.

3.6. Differential pressure drop

Differential pressure drop across the sectionalizing plate was measured to quantify the contribution of the energy dissipation rate near the sectionalizing plate to the overall process of mixing which depends on the total energy available for the liquid phase motion i.e. the average liquid phase circulation and the intercell exchange velocities; the values are reported in Table 5 for both the sparger.

It is clear from the values of the pressure drop that the pressure drop across the sectionalizing plate increase with an increase in the V_G . This indicates that the energy dissipation rate has gone up in the vicinity of the sectionalizing plates, but this increased energy dissipation has partially been used for the process of the bubble break-up and the balance for the liquid motion resulting into increased liquid circulation, which would also result in an increase in the u_B and a subsequent decrease in the mixing time as observed.

The differential pressure drop was found to be independent of the actual hydrostatic head acting on the sectionalizing plate. This suggests that the increase in H_c/D , the contribution of the pressure drop to the overall mixing process would be marginal, yet we observed some effect. One of the possible reason, could be the presence of the gas pockets (formed below the sectionalizing plates) causing an increase in the ε_G and yet does not contribute significantly to the energy dissipation rate at gas–liquid interface as this gas pocket has a much lower interfacial area as compared to the dispersed bubbles. Thus, in reality, even though the measured ε_G is higher, the energy available for the liquid motion could still be higher due to the reduced energy dissipation at the gas–liquid interface, resulting into higher liquid circulation velocities and also increased values of u_B .

With a decrease in the free area of the sectionalizing plate from 23 to 4%, there is an increase in the differential pressure drop from 5 to 25% at a constant V_G . The possible reason for the increase in the pressure drop could be the resistance offered by the hole for the gas flow. The decrease in the % FA of the sectionalizing plate ultimately decreases the intercell exchange velocity causing an increase in the mixing time.

It is clear that the sparger free area does not affect the pressure drop across the sectionalizing plates.

4. Conclusions

1. Extensive data has been collected of the mixing time variation in a sectionalized bubble column incorporated with sieve plate internals and it has been observed that mixing time decreases with an increase in the superficial gas

velocity and percent free area of the sectionalizing plate, whereas it increases with an increase in the H_c/D ratio.

2. Mixing time data in the presence of electrolyte have also been collected and the effect of periodic tracer addition has been discussed. The presence of electrolytes is observed to increase the mixing time due to an alteration in the fractional gas hold-up behavior.
3. The compartment model with single compartment per section has been found to be successful in predicting the variation in the local time dependent tracer concentration and also the final mixing time behavior.
4. For a given change in the sparger free area, no significant change has been observed in the mixing time and the fractional gas hold-up.
5. Empirical correlation has been proposed to estimate the fractional gas hold-up, mixing time, liquid phase dispersion coefficient and intercell exchange velocity as a function of the operating and the geometrical parameters for a sectionalized and non-sectionalized bubble column.

References

- [1] B.N. Thorat, J.B. Joshi, Regime transition in bubble column: experimental and prediction, *Exp. Therm. Fluid Sci.* 28 (2004) 423–430.
- [2] R. Krishna, A.J. Dreher, M.I. Urseanu, Influence of alcohol addition on gas hold-up in bubble columns: development of a scale up model, *Int. Comm. Heat Mass Transfer* 27 (4) (2000) 462–472.
- [3] R. Krishna, J. Ellenberger, C. Maretto, Flow regime transition in bubble columns, *Int. Comm. Heat Mass Transfer* 26 (4) (1999) 467–475.
- [4] A.B. Pandit, P.R. Gogate, V.Y. Dindore, Effect of tracer properties (volume, density and viscosity) on mixing time in mechanically agitated contactors, in: *Proceedings of the Tenth European Conference on Mixing*, 2000, pp. 385–393.
- [5] J.B. Joshi, U. Parasu Veera, V. Prasad, D.V. Phanikumar, N.S. Deshpande, S.S. Thakre, B.N. Thorat, Gas hold-up structure in bubble column reactors, *PINSA* 64A (1998) 441–567.
- [6] G.R. Kasat, A.B. Pandit, Mixing time studies in multiple impeller agitated reactors, *Can. J. Chem. Eng.* 82 (2004) 892–904.
- [7] J.B. Joshi, Axial mixing in multiphase contactors: a unified correlation, *Trans. Inst. Chem. Eng.* 58 (1980) 155–165.
- [8] A.B. Pandit, J.B. Joshi, Mixing in mechanically agitated gas–liquid contactors, bubble columns and modified bubble columns, *Chem. Eng. Sci.* 32 (8) (1983) 1189–1215.
- [9] M. Ravinath, G.R. Kasat, A.B. Pandit, Mixing time in a short bubble column, *Can. J. Chem. Eng.* 81 (2003) 185–195.
- [10] W.D. Deckwer, *Bubble Column Reactors*, Wiley, New York, 1992.
- [11] Y. Ohki, H. Inoue, Longitudinal mixing of the liquid phase in bubble column, *Chem. Eng. Sci.* 25 (1970) 1–16.
- [12] A. Kemoun, N. Rados, F. Li, M.H. Al-Dahhan, M.P. Dudukovic, P.L. Mills, T.M. Leib, J.J. Lerou, Gas holdup in a trayed bubble column, *Chem. Eng. Sci.* 56 (2001) 1197–1205.
- [13] A.J. Dreher, R. Krishna, Liquid-phase back mixing in bubble columns, structured by introduction of partition plates, *Catal. Today* 69 (2001) 165–170.
- [14] B.G. Kelkar, S.R. Phulgaonkar, Y.T. Shah, The effect of electrolyte solutions on hydrodynamic and back mixing characteristics in bubble columns, *Chem. Eng. J.* 27 (1983) 125–133.
- [15] J.M. Van Baten, R. Krishna, Scale up studies on partitioned bubble column reactors with the aid of CFD simulations, *Catal. Today* 79–80 (2003) 219–227.
- [16] R.W. Field, J.F. Davidson, Axial dispersion in bubble column, *Trans. Inst. Chem. Engrs.* 58 (4) (1980) 228–236.
- [17] F. Yamashita, Effect of ratio of aerated area of the partition plates on gas holdup in bubble column with partition plates, *J. Chem. Eng. Jpn.* 27 (3) (1994) 418–420.
- [18] J. K. De, *Studies in visbreaking*, M. Chem. Eng. thesis, Mumbai University, 1999.